

Showcasing research of the Hybrid research group Biopolymer and Recycling Innovations - HyBRIt - of the University of Groningen and NHL Stenden University of Applied Sciences, The Netherlands.

The effect of size and delignification on the mechanical properties of polylactic acid (PLA) biocomposites reinforced with wood fibres *via* extrusion

This research investigates the influence of alkaline treatment on wood fiber-reinforced wood-plastic composites (WPCs). The study examines the effects of fiber length, coupling agent, and structural changes resulting from the treatment. Results indicate improved mechanical properties, including increased tensile and flexural moduli, with the addition of a coupling agent. However, alkalinized fibers show lower performance due to the removal of hemicellulose and lignin during extrusion. The research contributes to sustainable, biobased materials and aligns with UN goals for resource conservation and waste management.

As featured in:



See Renato Lemos Cosse *et al.*, *RSC Sustainability*, 2023, 1, 876.

Cite this: *RSC Sustainability*, 2023, 1, 876

# The effect of size and delignification on the mechanical properties of polylactic acid (PLA) biocomposites reinforced with wood fibres via extrusion

Renato Lemos Cosse,<sup>a</sup> Vincent S. D. Voet,<sup>b</sup> Rudy Folkersma<sup>b</sup> and Katja Loos<sup>a</sup>

Natural fibres are promising candidates for polymer reinforcement due to their specific properties and renewability. To investigate the influence of wood fibre (WF) alkaline treatment on the mechanical properties of wood-plastic composites (WPCs), alkalis and raw WF-reinforced polylactic acid composites (40/60 wt%) were compounded using two different lengths of WF (100 and 400  $\mu\text{m}$ ) in the presence of maleic anhydride as the coupling agent. The structural analysis confirmed the removal of lignin and hemicellulose components from the fibres. The reinforcement increased the tensile and flexural moduli up to 140% and 137%, respectively, in the presence of a coupling agent. For raw fibre-reinforced composites, the tensile and flexural strengths increased by 12% and 12%, respectively. In contrast, alkalis fibres showed inferior performance, suggesting that the removal of hemicellulose and lignin added to the shear forces during extrusion led to their mechanical loss. Although all composites showed a decreased impact strength, the short fibre composites increased their properties by adding maleic anhydride. It can be clearly shown that short fibre-reinforced PLA performed mechanically better than the long counterparts and that the alkaline treatment did not produce better outcomes than the pristine raw fibres.

Received 26th January 2023  
Accepted 16th April 2023

DOI: 10.1039/d3su00039g

rsc.li/rscsus

## Sustainability spotlight

The depletion of oil resources instigates the search for a new alternative to fossil-based products. This work focuses on reinforcing biobased and biodegradable polylactic acid by adding wood fibres by conventional manufacturing methods. Natural fibres are widespread, and their use requires innovative solutions to the production sector (UN goals 9 and 12) besides mitigating the solid waste problem. The aim is to manufacture high-quality polymer products that can either be reintegrated to the production chain or the environment, meeting UN goals 14 and 15. In this direction, the present work contributes to the circular economy by using local raw materials from renewable sources.

## Introduction

Concerns about the depletion and better management of natural resources have instigated the search for materials that follow a circular economy concept.<sup>1</sup> Due to their biomass origin and biodegradability, natural fibres have shed a positive light on replacing conventional fibres, such as carbon or glass fibres, in composites. Synthetic fibres have a high carbon footprint, relying on nonrenewable resources. Natural fibres are low in cost, renewable, low density, abundant, less abrasive, less harmful to health, and less energy is needed for their processing.<sup>1,2</sup> In addition to these outstanding characteristics, many lignocellulosic fibres are biomass byproducts of the crop

harvesting and wood industry, and their incorporation in composites reduces the waste generated by agricultural activities.

The first occurrence of natural fibre reinforcing composites (NFCs) dates back to the 1930s when cotton fabric was impregnated with phenolic resin to supply the transportation industry.<sup>3</sup> In the following years, thermosets were widely applied in composites, but plant fibre reinforcement lost attractiveness due to water absorption, nonhomogeneous properties and the development of synthetic fibres. Thermoset resins are widely applied for natural fibre composites due to their high mechanical properties, chemical temperature resistance, and different processing possibilities fitting several geometric requirements. However, due to their crosslinks, thermosets are not directly reprocessable, hindering the life of closed-loop products.<sup>4</sup> On the other hand, polylactic acid (PLA) polyester is a biodegradable thermoplastic under industrial composting conditions<sup>5</sup> with relatively low cost and high mechanical performance that can be reprocessed and returned

<sup>a</sup>Macromolecular Chemistry and New Polymeric Materials, Zernike Institute for Advanced Materials, University of Groningen, Nijenborgh 4, Groningen, 9747 AG, The Netherlands. E-mail: k.u.loos@rug.nl

<sup>b</sup>Circular Plastics, NHL Stenden University of Applied Sciences, Van Schaikweg 94, Emmen, 7811 KL, The Netherlands



to the production chain, closing the production loop. The polyester can be processed through the same techniques applied to polyolefins (*e.g.*, extrusion, injection moulding, *etc.*), in addition to the advantage of being derived from renewable resources, such as potato, corn, sugar beet, *etc.*<sup>6,7</sup> Fibres reinforcing PLA are an alternative to enhance the mechanical properties of the polymer. When wood fibres are added to thermoplastic, they are called a wood-plastic composite (WPC). Similar to polyolefins, PLA shares the drawback of a flawed mechanical and chemical anchoring system with natural fibres due to the polymer's hydrophilicity in contrast to the fibres' hydrophilicity.<sup>7</sup>

Different physicochemical procedures, such as silanisation, acetylation, alkanisation or steam explosion, have been applied to alter the fibre's surface to enhance fibre dispersion and fibre/polymer adhesion. Among the procedures mentioned above, alkanisation is a cost-effective widespread chemical method for natural fibre-reinforced polymer composites. It washes out components of the fibres, such as lignin, hemicellulose, wax and oil, developing a rougher surface and enhanced aspect ratio.<sup>8</sup> These two features lead to better mechanical interlocking that improves the fibre/matrix interfacial adhesion in the resulting composites. After the alkaline treatment, the remaining component is cellulose microfibrils with remarkable tensile strength.<sup>8</sup> The microfibrils organise as strong thread-like structures whose crystallite arrangements form through hydrogen bonding. The hydroxyl group in natural fibres (fibre-cell-O-Na) is more readily ionised when aqueous sodium hydroxide (NaOH) is added to the treatment solution.<sup>9</sup>

Additionally, modifying the polymer matrix may provide a practical method for interfacial modification. To do this, a reactive moiety that later reacts with the fibres can be grafted onto the polymer matrix. Because of its low toxicity, ease of handling, and lack of tendency towards homopolymerisation under conventional free-radical melt-grafting conditions, maleic anhydride (MA) is typically the graft moiety of choice

when assigning reactivity to otherwise nonreactive polymers. The mechanism is explained in the following way. First, an initiator of dicumyl peroxide induces the formation of primary free radicals in the PLA chains. The free radicals then react with the unsaturated carbon-carbon link in the structure of MA, producing PLA-g-MA. And the anhydride groups in PLA-g-MA can create ester bonds with the hydroxyl groups in starch. In addition, the carboxylic groups resulting from the hydrolysis of MA's anhydride can create hydrogen bonds with the hydroxyl groups on the surface of wood flour. MA serves as a "bridge" between wood flour and the PLA matrix. Due to the crosslinking between wood flour and PLA generated by the reaction with MA, the interfacial adhesion of PLA and wood flour is significantly enhanced.<sup>10,11</sup> Generally, maleic anhydride grafting to PLA is carried out in an extruder using peroxides as the initiator in a process known as reactive extrusion (REX).<sup>12,13</sup> Twin-screw extruders can be used as an efficient reactor where grafting quickly takes place while the developed shear force distributes the reinforcement in the polymer matrix. It is a cost-effective solvent-free technique that has a short production time suitable for mass production.<sup>14,15</sup>

Murayama *et al.* evaluated the effects of wood fibre size distribution on polypropylene mechanical behaviour processed in a twin-screw extruder, concluding that fibres with a high aspect ratio enhanced tensile strength, while the impact strength decreased.<sup>16</sup> Teuber *et al.* analysed the dynamic particle degradation during compounding and reported fibre reduction throughout processing with high fibre content.<sup>17</sup> The influence of the kind of plant fibre on the mechanical properties of biocomposites was reported by Feng *et al.*<sup>18</sup> Wu *et al.* concluded that adding maleic anhydride as coupling agent led to the improvement of alkalised sisal fibres reinforcing maleated PP, and the flexural strength of the composite and the final fibre morphology influenced the mechanical properties.<sup>19</sup>

Although natural fibre composites have been reported under the influence of alkaline treatment and extrusion, there are few

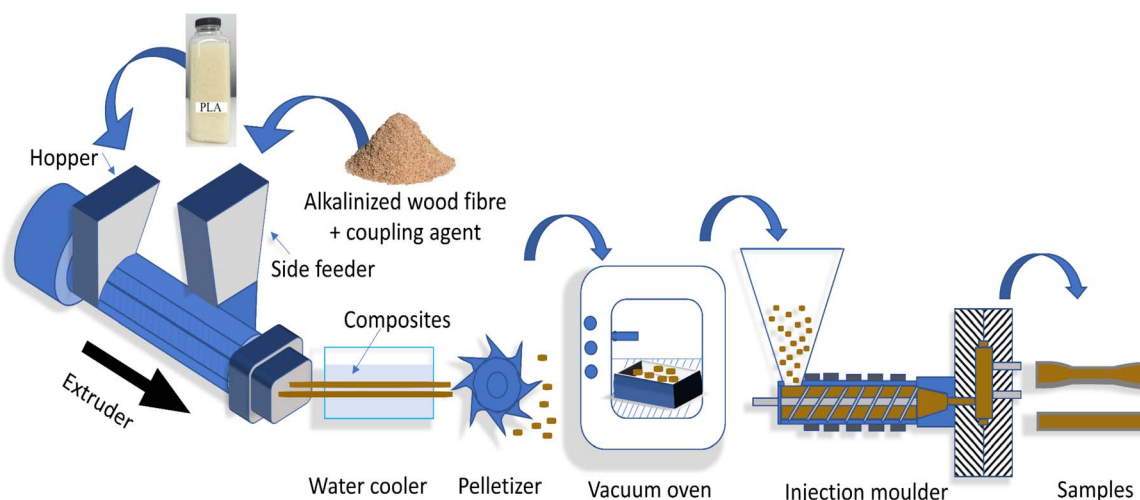


Fig. 1 Schematic representation of the composite manufacturing route, including compounding throughout a twin-screw extruder, water cooler, palletisation, drying and injection moulding.



works of those techniques when wood fibres (or flour) reinforce PLA and are posterior injection moulded. The present research aims to fill this gap by investigating the final thermal, mechanical and rheological properties of alkalis wood fibre-reinforced PLA manufactured by extrusion followed by injection moulding. For this purpose, wood fibres from hardwood and softwood were investigated in the interval of 32–400  $\mu\text{m}$ . Alkalis fibres were fed into the extruder and mixed with PLA throughout a reactive extrusion, using maleic anhydride as a coupling agent and dicumyl peroxide as an initiator. Fig. 1 shows the composite manufacturing route. The effects of alkaline treatment on the fibre structure were investigated by scanning electron microscopy (SEM) and Fourier transform infrared spectroscopy (FTIR). Our WPCs were evaluated by mechanical properties, morphology, heat deflection temperature (HDT), water absorption and rheological behaviour.

## Experimental

### Materials

Pellet-type PLA (IngeoTM Biopolymer 4043D, Nature Works) was used as the matrix. Two different size ranges of wood fibres were added to investigate the effects on the composite, Arbocel C100 (32–100  $\mu\text{m}$ ) and C400 (100–400  $\mu\text{m}$ ), both purchased from J. Rettenmaier & Söhne.

For fibre delignification, 99% water-free NaOH was acquired from De Parel, and 30% hydrochloric acid (HCl) was purchased from Bleko Chemie. A coupling agent was added to the processing to improve the wettability between the matrix and filler. For this purpose, maleic anhydride (MA) (95%, Sigma Aldrich) was added to the compounding in the presence of dicumyl peroxide (DCP) (Perkadox BC-FF, AkzoNobel), which acts as the initiator of the grafting reaction. Calcium carbonate (Omyalite®

50H) was purchased from Omya International AG to maintain the workable weight threshold of the coupling mixture gravimetric feeder.

### Chemical treatment of the wood fibres

To remove lignin and hemicellulose from the wood fibres, a 4 wt% NaOH solution was prepared with demineralised water, in which wood fibres were soaked and stirred for two hours at room temperature. Then, a 9.46 M HCl solution was used to neutralise the treated fibres. The resultant slurry was filtered, and the treated fibres were dried in a vacuum oven at 80 °C for five days until no significant weight difference was observed. The treated fibres underwent FTIR and SEM to evaluate the effect of the alkaline treatment.

### Compounding of WPCs

Prior to processing, PLA was dried at 70 °C for 24 hours in a vacuum oven. CaCO<sub>3</sub>, DCP, and MA were manually tumble-mixed (hereafter called the coupling mixture) and introduced into a gravimetric feeder. All specimens (Table 1) were prepared using a corotating twin extruder Kraus-Maffei Berstorff ZE25AX43D UTX, fed by three gravimetric feeders, each corresponding to PLA, WF and coupling mixture. PLA was added to the extruder hopper, while WF and the coupling agent were fed through the side feeder. The temperature profile of the extruder was 45, 150, 200, 180, 180, 180, 180, and 175 °C from the hopper to the die. At the same time, the screws of the side feeder and extruder were set at a speed of 200 rpm to produce extrudate strands that were immediately water cooled and pelletised.

The resulting pellets were dried at 75 °C for 72 hours. Then, in a 30 mm cylinder injection mould machine (Engel E-mac 50) with four heating zones (165, 170, 180 and 180 °C), samples were injected at 800 bar into a 35 °C mould at a cooling time of

Table 1 Description of specimen formulation

Specimen code	PLA (wt%)	WF (wt%)				Coupling mixture (correspond to 1 phr of the composite)		
		C100		C400		CaCO <sub>3</sub> (part)	DCP (part)	MA <sup>a</sup> (part)
		Raw	NaOH	Raw	NaOH			
PLA	100							
PLAc						10		
PC1R	60	40						
PC1R2	60	40				10	1	2
PC1R3	60	40				10	1	3
PC1R5	60	40				10	1	5
PC1N2	60		40			10	1	2
PC1N5	60		40			10	1	5
PC4R	60			40				
PC4R2	60			40		10	1	2
PC4R3	60			40		10	1	3
PC4R5	60			40		10	1	5
PC4N	60				40			
PC4N2	60				40	10	1	2
PC4N3	60				40	10	1	3
PC4N5	60				40	10	1	5

<sup>a</sup> The final MA levels in the composite are 0.15, 0.21, and 0.31%, corresponding to 2, 3, and 5 parts of the coupling mixture, respectively.



30 s. The samples were tested for tensile stress (ISO 527), Charpy impact unnotched (ISO 179-2), three-point bend (ISO 178), and heat deflection temperature (HDT).

### Characterisation

Tensile tests were performed on a Zwick UPM ZMART. PRO 14740. It ran according to ISO 527 using a load cell of 100 kN. The test speed for measurement of the tensile modulus was 1 mm min<sup>-1</sup>; then, the speed was increased to 5 mm min<sup>-1</sup> for measuring the stress–strain curve.

The flexural test was performed on a Zwick UPM ZMART. PRO 14740 using a 5 kN load cell varying the speed test from 2 mm min<sup>-1</sup> for measuring the tensile modulus to 10 mm min<sup>-1</sup>.

Charpy impact tests were carried out with Zwick PSW using a 4 Joules hammer to achieve 30–70% energy absorption following ISO 179-2 for unnotched specimens.

The heat deflection temperature (HDT) test was performed on an Instron HVS filled with silicone oil according to ISO 75-2 method A on an Instron HVS filled with silicone oil. The specimens were submitted to 1.8 MPa stress under increasing temperature.

NaOH-modified fibres were characterised using an FTIR spectrometer (Nicolet Summit Pro, ThermoFischer), scanning from 4000 to 400 cm<sup>-1</sup> at a resolution of 0.45 cm<sup>-1</sup> with 16 scans. Thermogravimetric analysis (TGA) was carried out to evaluate the effect of the alkaline treatment on the wood fibres. The measurements were obtained on the TGA5500 (TA Instruments) under 50 ml min<sup>-1</sup> nitrogen gas flow from room temperature to 700 °C with 10 °C min<sup>-1</sup> of heating rate. The tensile fracture surface of the composites reinforced with treated and nontreated fibres was analysed using LYRA/TESCAN scanning electronic microscopy (SEM). First, the samples were Au-coated in a vacuum chamber; conductive carbon tape was used to glue them to the microscopy sample holder to prevent electronic charge formation. The images were captured by applying a voltage of 5 kV. A water absorption test was performed following ISO 62. Injection moulded 60 × 60 × 2 mm square samples were soaked in demineralised water for 24, 48 and 120 hours at 23 °C. The samples of each system were measured on a scale with four significant numbers, and the average value was taken into account. The rheological measurements were carried out in AR1500EX (TA Instruments) at 180 °C considering the linear viscoelastic region.<sup>20</sup> Parallel aluminium plates with a 20 mm diameter and 1800 μm gap were applied for the frequency sweep test ranging from 0.1 to 100 rad s<sup>-1</sup>.

## Results and discussion

### Chemical treatment of the fibres

The chemical structure of wood fibres before and after the alkaline treatment was analysed through FTIR. The absorbance spectra of the raw fibres (Fig. 2) show strong carbonyl and aldehyde stretching at 1730 cm<sup>-1</sup>. The absorbance at 1663 cm<sup>-1</sup> corresponds to the unconjugated and conjugated carbonyl bands of hemicellulose.<sup>21,22</sup> The signal at 1235 cm<sup>-1</sup> is related to



Fig. 2 FTIR curves (2000–500 cm<sup>-1</sup>) of raw and alkalinized fibres. Absorbance at 1730 cm<sup>-1</sup> corresponds to carbonyl and aldehydes, while at 1663 cm<sup>-1</sup> to conjugated and unconjugated carbonyl bands of hemicellulose. Absorbance at 1235 and 1155 cm<sup>-1</sup> corresponds to lignin constituents.

the guaiacyl ring breathing with CO stretching, and 1155 cm<sup>-1</sup> comprises guaiacyl and syringyl C–H bonds, which are lignin constituents.<sup>21,23,24</sup> The absence of the vibrations mentioned above, or their weak absorption, suggests the (partial) removal of hemicellulose and lignin after the alkaline treatment.

Thermal degradation of the alkalinized fibres was determined by TGA/DTGA (Fig. 3) and depicted the peak temperature where the events occur. After the initial mass loss due to water evaporation, subsequent degradation followed a single-step process (Fig. 3A). Without treatment, raw fibres start degrading at a higher temperature than their NaOH-treated counterparts. The alkaline treatment moved the peak degradation temperature from 370 °C to 317 °C. This was expected since the remaining cellulose is less thermostable than lignin.<sup>22,25</sup> The higher char mass indicates a higher cellulose content. Alkalinized fibres have higher char residue due to the absence of waxes (pectin), non-fibre stream tissues (hemicellulose)<sup>26</sup> and cementing substance (lignin).<sup>27</sup> It can be said that higher char residues indicate higher purity of the fibres.<sup>26</sup> Similar results were observed for other lignocellulosic materials.<sup>28–33</sup>

The influence of the fibres' chemical modification on their morphology is depicted through SEM micrographs (Fig. 4). Fig. 4A shows the fibre before the alkaline treatment, where it is compact, and the layers are packed with a smooth and homogeneous surface. On the other hand, after the alkaline treatment (Fig. 4B), the wood fibres presented cracks between the layers, and their surface was already rougher with the presence of small voids, indicating the removal of hemicellulose and lignin. The removal leads to fibrillation, enlarging the specific area of the fibres where the polymer can bond to the fibre.<sup>34</sup>

Silva *et al.* reported that alkaline solution was efficient not only in the dissolution of lignocellulosic constituents of macadamia nutshell fibre that triggered fibrillation but also in removing wax, oil and impurities, reducing the average length



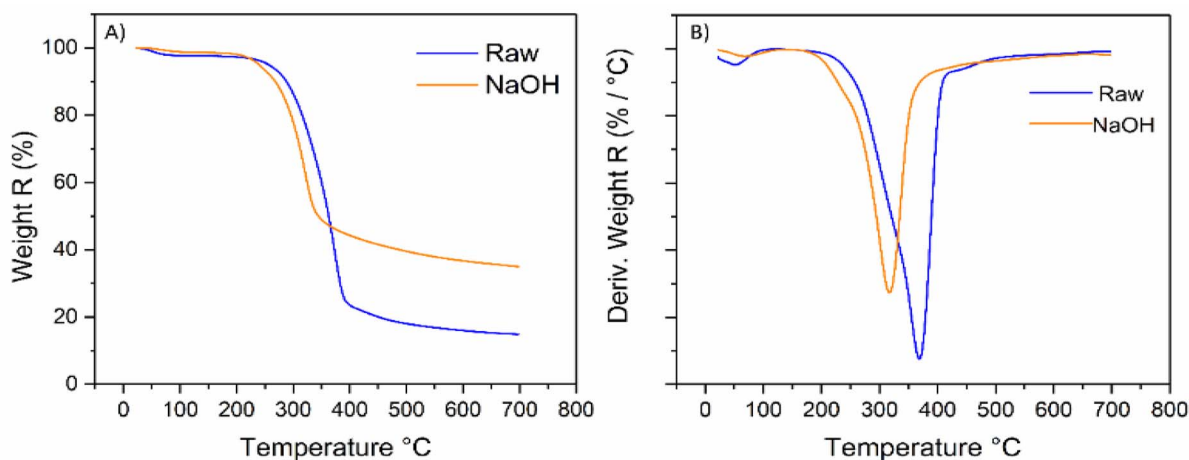


Fig. 3 (A) TGA, and (B) DTGA of raw fibres and alkaline treated fibres. Alkalinized fibres started degrading at lower temperature compared to raw fibres.

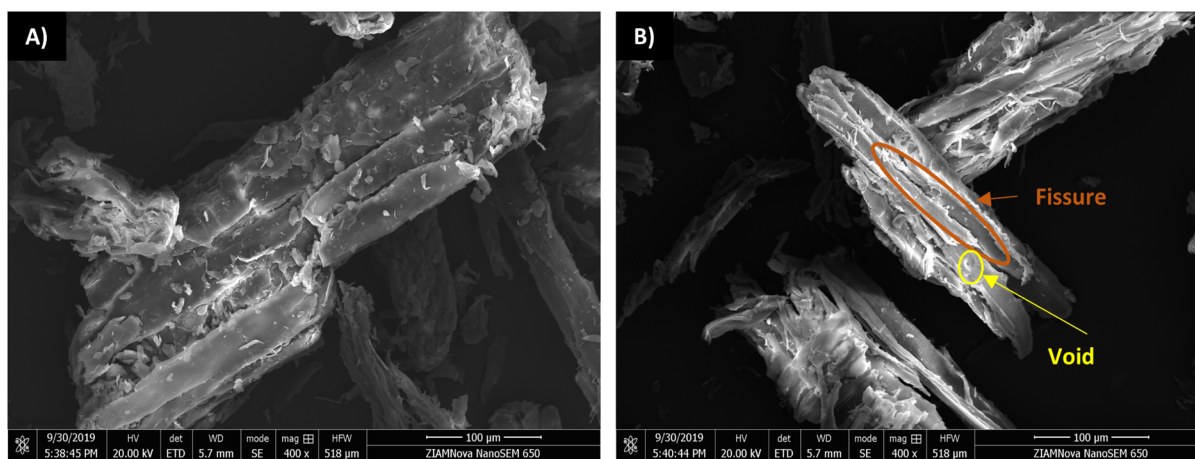


Fig. 4 SEM images of the raw fibre (A) which presents an even and smooth surface when compared to the fibre after alkaline treatment (B) that depicts fibrillation caused by the removal of lignin and hemicellulose, which was also responsible for the appearance of cracks and holes increasing the fibre surface area.

and radius of the fibres.<sup>35</sup> Olakanmi *et al.* highlighted that wood fibre treated at room temperature with an alkali concentration of up to 4 wt% achieved the isolation of cellulose.<sup>25</sup> In the present work, the degradation behaviour, chemical structure and morphology of the fibres corroborate the reports mentioned above, indicating the removal of hemicellulose and lignin from the wood fibres.

#### Mechanical properties of PLA/wood fibre composites

Fig. 5 shows the average tensile modulus and strength measurements for neat PLA compared to the raw and alkaline-treated wood fibre-reinforced composites. The addition of 40% wood fibre load in the composites increased the tensile modulus by at least 117% (8340 MPa) compared to neat PLA (3840 MPa) (Fig. 5A). The composite PC4R5 exhibited the highest tensile modulus (9250 MPa), while PC1N2 performed the lowest (7600 MPa). This suggests that wood fibre inherently

restricts polymer chain mobility. Previous works supported that conclusion, regardless of the selected mixing process (*e.g.*, extrusion, shear mixer).<sup>36,37</sup> Rigid fillers, such as calcium carbonate and wood fibres, have increased the tensile modulus of composites regardless of the contact interface.<sup>36–38</sup> The initial addition of the coupling mixture into the PLA/wood fibre composites was responsible for the tensile modulus decay when the opposite behaviour was expected. At the low level of MA, the tensile modulus values are not discernible, being in the error margin. The highest level of MA in the composites led to distinguishable tensile modulus behaviour when composites reinforced with longer fibres performed better than their short fibre counterparts.

Unlike the tensile modulus, the tensile strength of the composites showed a different behaviour among the specimens (Fig. 5B). Although adding wood fibre reduced the tensile strength of the composites (except for PC1R), a coupling agent was responsible for raw fibre-reinforced composites reaching



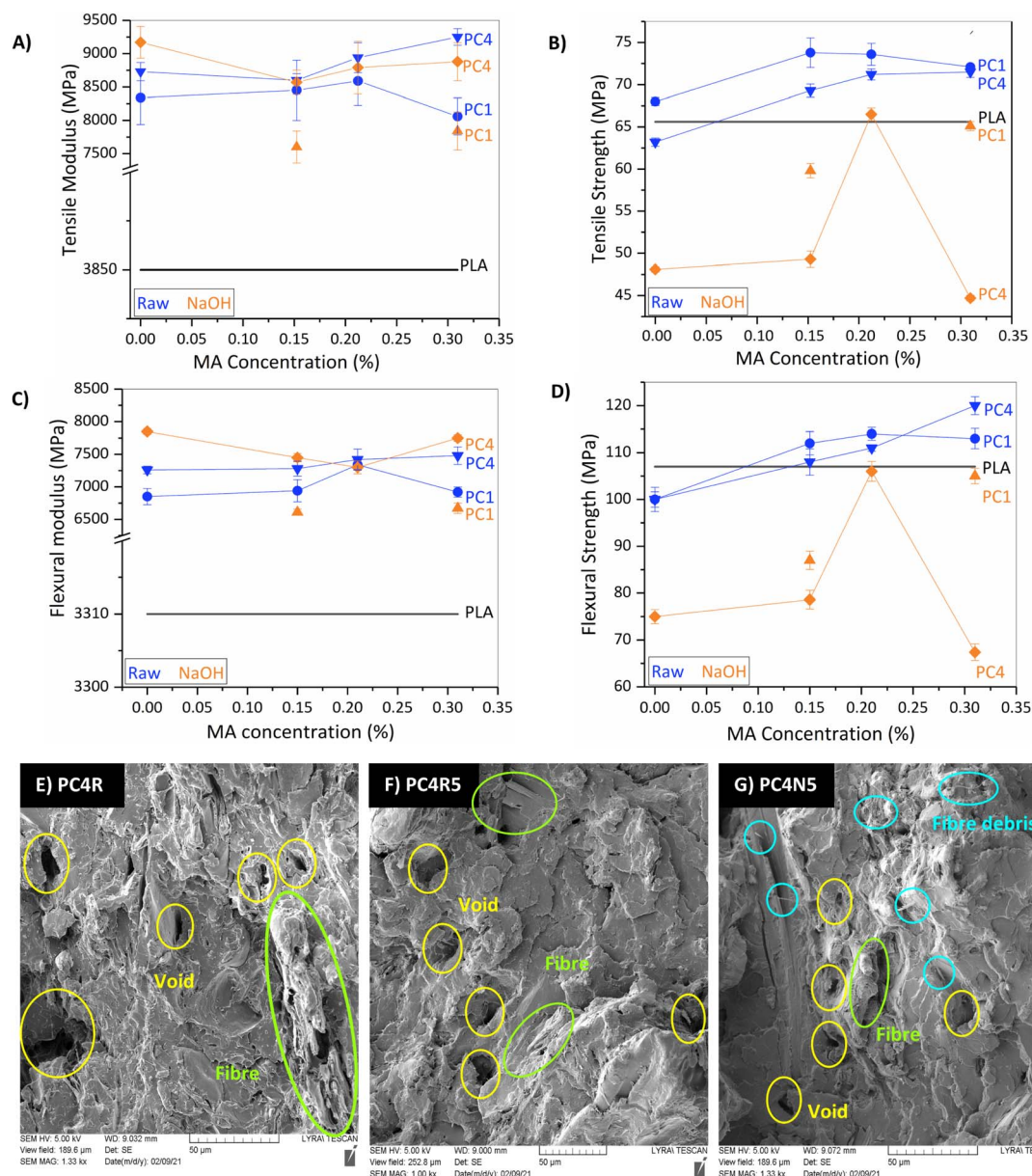


Fig. 5 (A) Tensile modulus, (B) tensile strength, (C) flexural modulus, (D) flexural strength, and SEM of the fracture surface of WPCs after tensile test. (E) PC4R; (F) PC4R5; (G) PC4N5.

values superior to neat PLA. The tensile strength of PC1R3 was 12% higher than that of PLA. This behaviour contrasts with the alkali counterparts that kept their performance inferior to that of neat PLA. Olakanmi *et al.* reported that fibres of similar average size washed in 4 wt% NaOH solution for 120 minutes demonstrated optimal tensile properties when compressed moulded with HDPE.<sup>25</sup> This indicates that the processing conditions strongly influence the resulting properties in addition to the fibre treatment parameters. For all composites, the coupling mixture delivered an initial better performance; however, the increment of MA levelled off or decreased tensile strength.

Fig. 5C and D depicts the flexural modulus and strength of the WPCs. The results of the flexural tests are similar to the

values presented from the tensile tests. The WPC flexural modulus (Fig. 5C) increased by at least 107% (6850 MPa) in the presence of wood fibres. The flexural modulus is more sensitive to adding longer fibres than the presence of the coupling mixture, with PC4N being 137% higher than PLA. On the other hand, fibre treatment influenced the flexural strength performance more than fibre size. Raw WF was responsible for the WPC's higher flexural strength since PC4R5 performed 12% higher than PLA.

Both tensile and flexural moduli were expected to increase since wood fibre is stiffer than the PLA matrix. Another contribution is that wood fibres restrain the movement of the polymer chain, decreasing the elongation at fracture. The data collection setup is essential to consider in analysing those properties.



Tensile and flexural modulus data come from the elastic region of the stress/strain curve of the WPC, which is far below the failure point. For this reason, the analysis neglects the influence of many fibre defects on the modulus of the composites. The tensile strength goes far beyond the elastic region of the stress/strain curve, which requires the synergistic work of the matrix and filler to avoid premature fracture. It is also known that only a certain concentration of graft copolymer is required to saturate the interface and produce optimum compatibilisation.<sup>39</sup> The excess of MA in the interface can lead to a decrease in tensile and flexural strength.<sup>10</sup> This behaviour is not depicted for the PC4R5, showing the highest flexural strength. On the other hand, PC4N5 depicted the lowest tensile and flexural strength. It is reported that thermoplastic grafted with MA in the presence of alkali metal (reminiscent of the salt formed from the neutralisation reaction of fibre treatment) at a high temperature can form a crosslinked structure, leading to a third phase in the composite with different characteristics.<sup>40</sup> However, further studies are necessary to evaluate the occurrence of these events, which is out of the scope of this present work.

Fig. 5E–G show SEM images from the fractured surface of the composites after the tensile tests. In general, a lack of wettability of the wood fibres by the matrix was observed. Voids in the fracture surface indicate the filler's pullout, which can be either CaCO<sub>3</sub> or wood fibres. As soon as the coupling agent mixture was added to the compound, it reduced the fibre size. Fig. 5G shows the high presence of fibre debris on the fracture surface that can work as stress concentration points, having a deleterious effect on the tensile and flexural strength. It is well known that the shear forces developed by the extruder screw are responsible for damaging the cellulosic component; additionally, as CaCO<sub>3</sub> is stiff, it acts as an abrasive, wearing out the fibres. Removing fibre binders, such as hemicellulose and lignin, intensified fibrillation, leading to low shear resistance.

The comparative impact performance of the raw and NaOH-treated fibres is depicted in Fig. 6. Incorporating WF into the

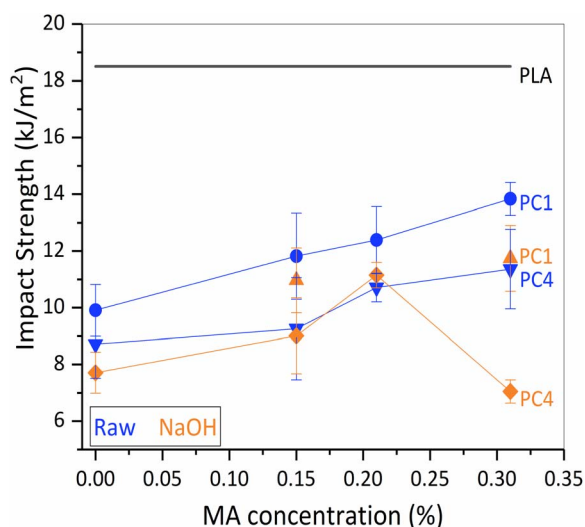


Fig. 6 Impact Strength of PLA, raw and alkalised WPCs.

PLA matrix decreased the impact resistance of all composites compared to neat PLA. However, the increase in maleic anhydride content elevated the average impact strength of all composites except PC4N5, which contained 0.31% MA.

Untreated PC1 composites showed the highest impact strength in comparison to their counterparts. The lower impact strength performance of the composites was attributed to the stress concentration points caused by the filler embedded within the polymeric matrix and the relative brittleness of the WF compared to PLA. The stress points become weak spots from where cracks quickly initiate and propagate compared to the neat PLA. The matrix nature highly influences stress propagation. Yuan *et al.* reported that in addition to PLA brittleness, maleic anhydride lowers the molecular weight of PLA and decreases its crystallinity.<sup>41</sup> Furthermore, WF from softwood has a fibril angle that is attributed to its high elastic modulus and low elongation at break, suggesting a relatively low impact performance.<sup>11,42</sup>

Another way to investigate the performance of composites is through HDT. It is an essential parameter in the design of many products because it indicates the highest temperature to which a polymer can be subjected without undergoing significant physical deformations at a given load. Fig. 7 summarises the obtained results for the heat deflection temperature (HDT). This shows that fibre incorporation was responsible for increasing the thermomechanical properties. The increase in coupling mixture level has a negligible effect on HDT. HDT is highly dependent on the modulus; since the tensile and flexural moduli increase for the composites, the HDT was expected to increase, meaning a decrease in the creep rate under a given load. However, there was a decay of the HDT for alkalised fibre-reinforced PLA compared to raw fibre-reinforced PLA. Liu *et al.* reported that decreased fibre length triggered a decrease in HDT. Alkaline treatment leads to the reduction of fibre length by lignin and hemicellulose removal.<sup>43</sup> In addition, the morphology analysis of the surface fracture shows debris resulting from fibre fibrillation after compounding.

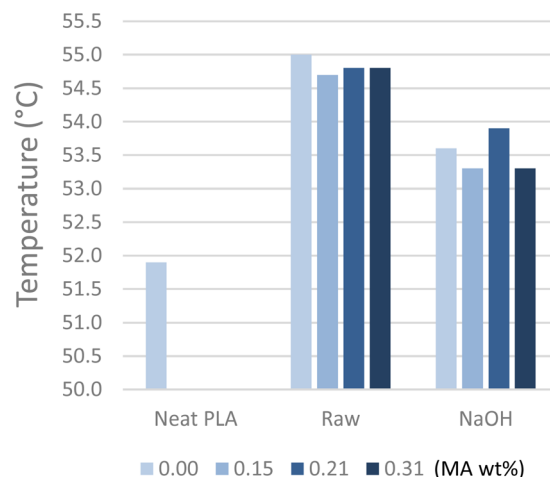


Fig. 7 HDT of PLA and WPCs reinforced with C400 fibres.





### Water absorption of WPCs

Neat PLA and wood plastic composites were soaked in demineralised for 24, 48, and 120 hours. The increase in the sample mass has been registered in Fig. 8. PLA absorbed less water than all the composites, showing almost no significant mass increase. On the other hand, wood plastic composites increased their mass continuously over time. This confirms the hydrophobicity of this polymer matrix, addressing the WPCs' higher water content to the wood fibres' hydrophilicity. Alkalised fibres reinforcing PLA did not mitigate the water absorption effect; they increased the absorption, except for PC4N5, which had a lower mass than PC4R5. In addition to the fibre load and the composite's structural arrangement, water absorption depends on the particle size. In general, the PC4 composites retained more water than their PC1 counterparts.

The maleic anhydride level was not practical in reducing the water absorption of the composites. In contrast to the performance of the studied WPCs, MA leads to the crosslinking of macromolecules, increasing the internal regularity of the

composites and reducing the space where water can penetrate.<sup>11</sup> The fibre load and particle geometry dominated the water absorption of the system. Kaboorani reported that large wood particles increased the water absorption rate in wood plastic composites.<sup>44</sup> Yeh *et al.* observed no moisture reduction for NaOH-treated fibres.<sup>45</sup> This corroborates the predominantly higher water absorption for composites containing long fibres with no anchoring effect of the matrix/fibre.

### Rheology

Fig. 9A shows the complex viscosity and storage modulus results from the oscillatory frequency sweep test for PLA and WPCs. Fig. 9A depicts that the increase in the angular frequency led to a decrease in all composites' complex viscosity, evidencing shear-thinning behaviour. The complex viscosity decay is a positive characteristic since less energy is required for processing the composite at higher shear rates (*e.g.*, 3D printing, extrusion, injection moulding). Shear-thinning behaviour has been reported for 20 and 30 wt% poplar fibres (<180  $\mu\text{m}$  up to

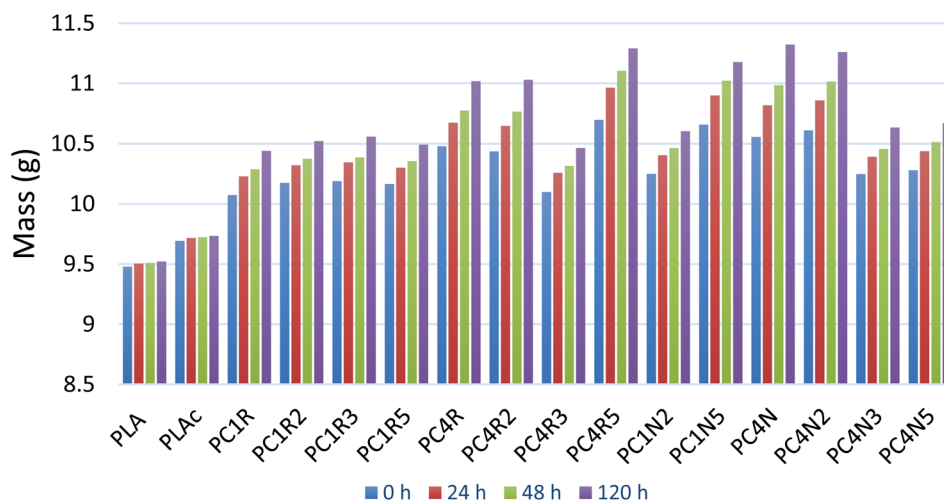


Fig. 8 Water absorption measurements for PLA and wood plastic composites over 24, 48, and 120 hours.

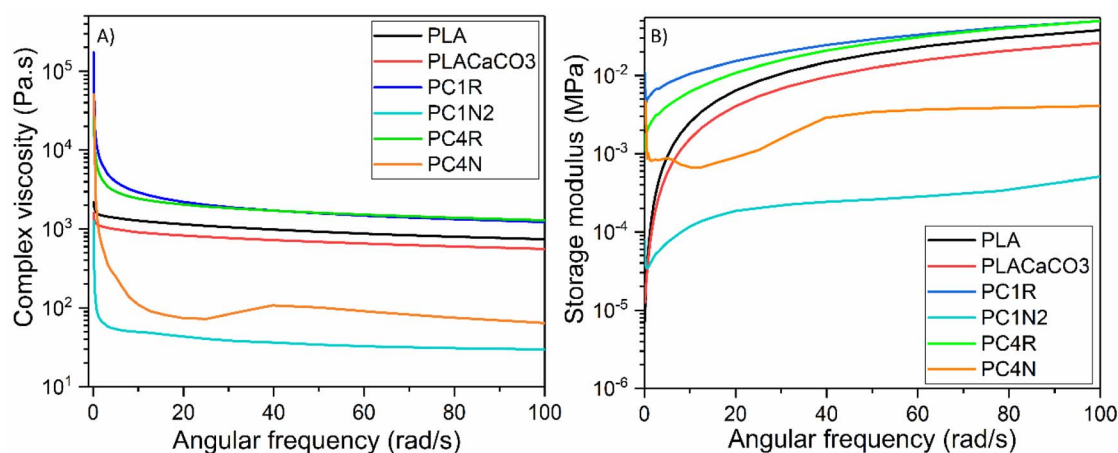


Fig. 9 (A) Complex viscosity obtained by frequency sweep. (B) Storage modulus obtained from frequency sweep test.



2360  $\mu\text{m}$ ) reinforcing PLA.<sup>20,36</sup> Although the shear-thinning effect is present in PLA/WF and PLA, the latter is affected minimally. The higher complex viscosity of PLA/WF at the lowest angular frequency corroborates the trends in the tensile and flexural tests. Although all composites show a steep decrease in the complex viscosity with minimal angular frequency increment, raw fibre-reinforced PLA is kept higher than neat PLA. PC1R presented the highest complex viscosity from 0.1 to 40  $\text{rad s}^{-1}$  angular frequency. At higher angular frequencies, raw fibres showed no considerable difference in complex viscosity when comparing short and long fibres.

On the other hand, the complex viscosity of the NaOH-treated fibre immediately becomes lower than that of PLA when the angular frequency increases. This indicates the loss of the structural arrangement of wood fibre by removing hemicellulose and lignin. The removal leads to fibrillation and a decreased aspect ratio, lowering viscosity by reducing fibre-fibre topological contact.<sup>42,46</sup>

The storage modulus of all composites in Fig. 9B at 0.1  $\text{rad s}^{-1}$  is higher than that of neat PLA. This indicates good fibre dispersion in the polymer matrix during processing. The storage modulus of the raw reinforced fibre reinforcing PLA matrix is the highest, with the shorter fibres having the highest values. Short fibres may present fewer defects than long fibres.<sup>29</sup> Alkaline treatment partially removed the natural binder of the fibres, lignin, leading to fibrillation. Researchers observed that the probability of organised network formation by rod-like structures (similar to untreated wood fibres) is higher than that of inherent fibrillated structures, as shown in the morphology analysis of alkalisated fibres.<sup>47</sup> The absence of an organised network makes the alkalisated fibres reinforcing PLA less resistant to flow. The storage modulus of PC4N is higher than that of PC1N2, indicating that this amount of coupling agent was not as influential as the fibre geometry itself. However, more details about the agglomeration and packing effect of these fibrils can be explored in the future.

## Conclusions

Wood plastic composites containing 40 wt% raw and alkalisated wood fibres were manufactured by extrusion and injection moulding. First, an alkaline solution removed the hemicellulose and lignin from the wood fibres, as confirmed by FTIR, thermal and morphology analyses. Afterwards, tests registered higher mechanical performance for raw fibre-reinforced PLA. For this system, adding a coupling mixture increases the tensile strength and modulus up to 12% and 140%, respectively. The tensile and flexural moduli increased in the presence of fibres. Adding long raw fibres and MA to PLA increased the flexural strength to 12% and flexural modulus to 137% for NaOH-treated long fibres. The tensile and flexural modulus increase is reflected in higher HDT.

The impact strength of the composites decreased compared to that of PLA, and short fibres performed better than long fibres. Alkalisated fibres were responsible for the poor performance of the composites since the NaOH unpacked the fibres, and the shear forces of the processing fibrillated them,

weakening the lignocellulosic structure. The water absorption of the composites increased compared to that of PLA with negligible water uptake. The hydrophilicity of the WF dominated the water absorption rate of the wood plastic composites.

Rheological measurements indicated good wood fibre distribution in the matrix. However, NaOH treatment and extrusion fragmented the fibres, leading to their poor performance compared to their untreated counterparts. In general, the alkaline treatment of wood fibres was not beneficial for processing under high shear rates, such as extrusion and injection moulding.

## Author contributions

Renato L. Cosse: writing original draft, methodology, data curation. Formal analysis, investigation, conceptualisation, validation and visualisation. Vincent S. D. Voet: conceptualisation, validation, writing – review & editing. Rudy Folkersma: conceptualisation, validation, writing – review & editing, resources, funding acquisition. Katja Loos: validation, writing – review & editing, resources, funding acquisition.

## Conflicts of interest

There are no conflicts to declare.

## Acknowledgements

This work was supported by Greenwise Campus, Regio Deals, Province of Drenthe and Municipality of Emmen. The authors thank Corinne van Noordenne and Tobias van der Most for helping with the processing and mechanical tests and Jur van Dijken for the thermal and rheological tests.

## References

- 1 L. Mohammed, M. N. M. Ansari, G. Pua, M. Jawaid and M. S. Islam, *Int. J. Polym. Sci.*, 2015, **2015**, 1–15.
- 2 K. L. Pickering, M. G. A. Efendy and T. M. Le, *Composites, Part A*, 2016, **83**, 98–112.
- 3 C. Baley, A. Bourmaud and P. Davies, *Composites, Part A*, 2021, **144**, 106333.
- 4 V. S. D. Voet, J. Guit and K. Loos, *Macromol. Rapid Commun.*, 2021, **42**, 2000475.
- 5 W. Groot, J. van Krieken, O. Sliemers and S. de Vos, in *Poly(Lactic Acid): Synthesis, Structures, Properties, Processing, and Applications*, 2010, vol. 1, pp. 1–18.
- 6 A. F. Sousa, R. Patrício, Z. Terzopoulou, D. N. Bikiaris, T. Stern, J. Wenger, K. Loos, N. Lotti, V. Siracusa, A. Szymczyk, S. Paszkiewicz, K. S. Triantafyllidis, A. Zamboulis, M. S. Nikolic, P. Spasojevic, S. Thiyagarajan, D. S. van Es and N. Guigo, *Green Chem.*, 2021, **23**, 8795–8820.
- 7 P. F. Alao, L. Marrot, M. D. Burnard, G. Lavrič, M. Saarna and J. Kers, *Polymers*, 2021, **13**, 851.
- 8 T. Gurunathan, S. Mohanty and S. K. Nayak, *Composites, Part A*, 2015, **77**, 1–25.



- 9 K. M. F. Hasan, P. G. Horváth, M. Bak and T. Alpár, *RSC Adv.*, 2021, **11**, 10548–10571.
- 10 S. Lv, J. Gu, H. Tan and Y. Zhang, *J. Appl. Polym. Sci.*, 2016, **133**, 1–9.
- 11 L. Zhang, S. Lv, C. Sun, L. Wan, H. Tan and Y. Zhang, *Polymers*, 2017, **9**, 5–8.
- 12 L. Gardella, M. Calabrese and O. Monticelli, *Colloid Polym. Sci.*, 2014, **292**, 2391–2398.
- 13 H. Oliver-Ortega, R. Reixach, F. X. Espinach and J. A. Méndez, *Materials*, 2022, **15**, 1161.
- 14 D. D. S. Morais, D. D. Siqueira, C. B. B. Luna, E. M. Araujo, E. B. Bezerra and R. M. R. Wellen, *Mater. Res. Express*, 2019, **6**, 055315.
- 15 S. Detyothin, S. E. M. Selke, R. Narayan, M. Rubino and R. Auras, *Polym. Degrad. Stab.*, 2013, **98**, 2697–2708.
- 16 K. Murayama, T. Ueno, H. Kobori, Y. Kojima, S. Suzuki, K. Aoki, H. Ito, S. Ogoe and M. Okamoto, *J. Wood Sci.*, 2019, **65**, 1–10.
- 17 L. Teuber, H. Militz and A. Krause, *Composites, Part A*, 2016, **84**, 464–471.
- 18 J. Feng, W. Zhang, L. Wang and C. He, *Bioresources*, 2020, **15**, 2596–2604.
- 19 C. Wu, S. Jia, R. Chen, Z. Huang, S. Zhai, Y. Feng, Z. Yang and J. Qu, *J. Reinf. Plast. Compos.*, 2013, **32**, 1907–1915.
- 20 X. Zhao, H. Tekinalp, X. Meng, D. Ker, B. Benson, Y. Pu, A. J. Ragauskas, Y. Wang, K. Li, E. Webb, D. J. Gardner, J. Anderson and S. Ozcan, *ACS Appl. Bio Mater.*, 2019, **2**, 4557–4570.
- 21 J. Gabhane, S. P. M. P. William, A. N. Vaidya, S. Das and S. R. Wate, *Waste Manage.*, 2015, **40**, 92–99.
- 22 H. Choe, G. Sung and J. H. Kim, *Compos. Sci. Technol.*, 2018, **156**, 19–27.
- 23 M. Frey, D. Widner, J. S. Segmehl, K. Casdorff, T. Keplinger and I. Burgert, *ACS Appl. Mater. Interfaces*, 2018, **10**, 5030–5037.
- 24 K. K. Pandey, *J. Appl. Polym. Sci.*, 1999, **71**, 1969–1975.
- 25 E. O. Olakanmi, E. A. Ogunesan, E. Vunain, R. A. Lafia-araga, M. Doyoyo and R. Meijboom, *Polym. Compos.*, 2016, **37**, 2657–2672.
- 26 M. K. Hossain, M. W. Dewan, M. Hosur and S. Jeelani, in *25th Technical Conference of the American Society for Composites and 14th US-Japan Conference on Composite Materials 2010*, 2010, vol. 1, pp. 79–96.
- 27 D. Puglia, M. Monti, C. Santulli, F. Sarasini, I. M. De Rosa and J. M. Kenny, *Fibers Polym.*, 2013, **14**, 423–427.
- 28 M. M. Kabir, H. Wang, K. T. Lau and F. Cardona, *Appl. Surf. Sci.*, 2013, **276**, 13–23.
- 29 N. Shanmugasundaram, I. Rajendran and T. Ramkumar, *Carbohydr. Polym.*, 2018, **195**, 566–575.
- 30 R. Vijay, A. Vinod, D. Lenin Singaravelu, M. R. Sanjay and S. Siengchin, *Int. J. Lightweight Mater. Manuf.*, 2021, **4**, 43–49.
- 31 S. C. Agwuncha, S. Owonubi, D. P. Fapojuwo, A. Abdulkarim, T. P. Okonkwo and E. M. Makhatha, in *Materials Today: proceedings*, Elsevier Ltd, 2021, vol. 38, pp. 958–963.
- 32 K. Obi Reddy, C. Uma Maheswari, M. Shukla, J. I. Song and A. Varada Rajulu, *Composites, Part B*, 2013, **44**, 433–438.
- 33 H. M. Nascimento, D. C. T. Granzotto, E. Radovanovic and S. L. Fávaro, *Composites, Part B*, 2021, **227**, 109414.
- 34 D. Ray, B. K. Sarkar, R. K. Basak and A. K. Rana, *J. Appl. Polym. Sci.*, 2002, **85**, 2594–2599.
- 35 N. G. S. Silva, L. I. C. O. Cortat and D. R. Mulinari, *J. Polym. Environ.*, 2021, **29**, 3271–3287.
- 36 X. Zhao, K. Li, Y. Wang, H. Tekinalp, G. Larsen, D. Rasmussen, R. S. Ginder, L. Wang, D. J. Gardner, M. Tajvidi, E. Webb and S. Ozcan, *ACS Sustain. Chem. Eng.*, 2020, **8**, 13236–13247.
- 37 A. Rahman, J. Fehrenbach, C. Ulven, S. Simsek and K. Hossain, *Ind. Crops Prod.*, 2021, **172**, 114028.
- 38 T. Boronat, V. Fombuena, D. Garcia-Sanoguera, L. Sanchez-Nacher and R. Balart, *Mater. Des.*, 2015, **68**, 177–185.
- 39 R. Zhu, H. Liu and J. Zhang, *Ind. Eng. Chem. Res.*, 2012, **51**, 7786–7792.
- 40 M. Ueda, S. Mizunuma, M. Oba and Y. Minoura, *J. Soc. Chem. Ind.*, 1968, **71**, 432–437.
- 41 Q. Yuan, D. Wu, J. Gotama and S. Bateman, *J. Thermoplast. Compos. Mater.*, 2008, **21**, 195–208.
- 42 L. T. T. Vo, J. Girones, C. Beloli, L. Chupin, E. di Giuseppe, A. C. Vidal, A. Soutiras, D. Pot, D. Bastianelli, L. Bonnal and P. Navard, *Ind. Crops Prod.*, 2017, **107**, 386–398.
- 43 W. Liu, L. T. Drzal, A. K. Mohanty and M. Misra, *Composites, Part B*, 2007, **38**, 352–359.
- 44 A. Kaboorani, *Constr. Build. Mater.*, 2017, **136**, 164–172.
- 45 S. K. Yeh, C. C. Hsieh, H. C. Chang, C. C. C. Yen and Y. C. Chang, *Composites, Part A*, 2015, **68**, 313–322.
- 46 M. C. Branciforti, H. S. Yang, I. Hafez, N. C. A. Seaton and W. T. Y. Tze, *Cellulose*, 2019, **26**, 4601–4614.
- 47 T. Mukherjee, N. Kao, R. K. Gupta, N. Quazi and S. Bhattacharya, *J. Appl. Polym. Sci.*, 2016, **133**, 43200.

